

NASA TECHNICAL
MEMORANDUM

NASA TM X-53296

July 19, 1965

NASA TM X-53296

N 65 - 32872
(ACCESSION NUMBER)
15
TMX-53296
(NASA CR OR TMX OR AD NUMBER)

FACILITY FORM 602
(PAGES)
1
(THRU)
1
(CODE)
31
(CATEGORY)

CONTROL FACTORS FOR APOLLO-SATURN 201 VEHICLE

by BILLY W. NUNLEY
Aero-Astrodynamics Laboratory

GPO PRICE \$ _____

CSFTI PRICE(S) \$ _____

Hard copy (HC) \$ 2.00

Microfiche (MF) .50

NASA

George C. Marshall
Space Flight Center,
Huntsville, Alabama

ff 653 July 65

NASA-GEORGE C. MARSHALL SPACE FLIGHT CENTER

TECHNICAL MEMORANDUM X-53296

CONTROL FACTORS FOR
APOLLO-SATURN 201 VEHICLE

By

Billy W. Nunley

ABSTRACT

32872

This report presents the control factor data to be used for Apollo-Saturn 201 vehicle control studies. Included are angular velocities, linear velocities, angular accelerations, and linear accelerations due to engine and aerodynamic forces. Also included are three-sigma variations of the more important control factors for the standard eight-engine case; i.e., no engine-out conditions were studied.

Author

NASA-GEORGE C. MARSHALL SPACE FLIGHT CENTER

TECHNICAL MEMORANDUM X-53296

July 19, 1965

CONTROL FACTORS FOR
APOLLO-SATURN 201 VEHICLE

By

Billy W. Nunley

DESIGN SECTION
AERODYNAMIC DESIGN BRANCH
AERODYNAMICS DIVISION
AERO-ASTRODYNAMICS LABORATORY

LIST OF ILLUSTRATIONS

<u>Figure</u>	<u>Title</u>	<u>Page</u>
1	Apollo-Saturn 201 Vehicle Configuration	14
2	Variation of Center of Gravity with Flight Time	15
3	Variation of Pitch and Yaw Moment of Inertia Versus Flight Time	16
4	Variation of Roll Moment of Inertia Versus Time	17
5	Variation of Stability Margin with Flight Time	18
6	Cant Angle Versus Time	19
7	Variation of Angular Accelerations Due to Aerodynamic Forces Versus Time	20
8	Variation of Angular Acceleration Due to Engine Forces with Time	21
9	Variation of Ratio of Gradients of Angular Acceleration Versus Time	22
10	Three-Sigma Variations of C_1 , C_2 , and C_1/C_2	23
11	Variation of Angular Acceleration in Roll Due to Engine Forces with Time	24
12	Variation of Linear Acceleration Due to Aerodynamic Forces Versus Time	25
13	Variation of Linear Acceleration Due to Engine Forces with Time	26
14	Variation of Resultant Axial Acceleration Due to Aerodynamic and Engine Forces Versus Time	27
15	Variation of Angular Velocities Due to Aerodynamic Forces Versus Time	28

LIST OF TABLES

<u>Table</u>	<u>Title</u>	<u>Page</u>
I	Nominal Trajectory Data	5
II	C_1 Variations	6
III	C_2 Variations	7
IV	C_1/C_2 Variations	8
V	Z_1/m Variations	9
VI	Z_2/m Variations	10
VII	$(Z_1/m)/(Z_2/m)$ Variations	11
VIII	$C_1/(Z_1/m)$ Variations	12
IX	$C_2/(Z_2/m)$ Variations	13

DEFINITION OF SYMBOLS

<u>Symbol</u>	<u>Definition</u>
A_0	$(M_2/I)y, z$ of one control engine for $\beta_{z,y} = 0^\circ$, rad/sec^2
B^o	$[\partial(M_2/I)y, z / \partial \beta_{z,y}]_{\beta=0^\circ}$ of one control engine, $(\text{rad/sec}^2)/\text{deg } \beta_{z,y}$
A_1	$(M_2/I)y, z$ of one fixed engine, rad/sec^2
$C_{1y,z}$	$\partial(M_1/I)y/\partial\alpha$ or $\partial(M_1/I)z/\partial\tau$: gradient through $\alpha = \tau = 0^\circ$ of angular acceleration about the pitch axis due to angle of attack, α , or about the yaw axis due to sideslip angle, τ , $(\text{rad/sec}^2)/\text{deg } \alpha$ or $(\text{rad/sec}^2)/\text{deg } \tau$
CG/D	distance between longitudinal reference point ¹ and missile center of gravity, calibers
CP/D	distance between longitudinal reference point ¹ and missile center of pressure, calibers
C_x	axial force coefficient (C_{D_0})
$C_{y\tau}$	gradient of side force coefficient ² due to angle of sideslip, $1/\text{deg } \tau$ or $1/\text{rad } \tau$, (also $dC_y/d\tau = Y/\tau qS$)
$C_{z\alpha}$	Gradient of normal force coefficient ² due to angle of attack, $1/\text{deg } \alpha$ or $1/\text{rad } \alpha$, (also $dC_z/d\alpha = Z_1/\alpha qS$)
D	reference diameter, inches or meters
d_e	external damping factor due to missile body, $(\text{rad/sec}^2)/(\text{rad/sec})$
d_i	internal damping due to fuel flow, $(\text{rad/sec}^2)/(\text{rad/sec})$
d_t	total damping factor, $(\text{rad/sec}^2)/(\text{rad/sec})$

¹The longitudinal reference point has been chosen as station 100.0 (gimbal station).

²For a symmetrical missile, $C_{y\tau} = C_{z\alpha}$.

DEFINITION OF SYMBOLS (Cont'd)

<u>Symbol</u>	<u>Definition</u>
F_s	standard thrust of one engine, kg
$(F - X)/m$	longitudinal acceleration ($F = nF_s$), m/sec ²
H^o	$[\partial(M_2/I)_x/\partial\beta_y, z]_{\beta=0^\circ}$ of one control engine, (rad/sec ²)/deg β_y, z
I_x	mass moment of inertia of the missile about the x-axis, kg-m-sec ²
$I_{y, z}$	mass moment of inertia of the missile about the y- or z-axis, kg-m-sec ²
J_o	Z_2/m of one control engine for $\beta = 0^\circ$, m/sec ²
K^o	$[\partial(Y_2, Z_2/m)/\partial\beta_y, z]_{\beta=0^\circ}$ of one control engine, (m/sec ²)/deg β_y, z
J_1	Z_2/m of one fixed engine, m/sec ²
M	Mach number or moment
m	mass of missile, kg-sec ² /m
M_x	rolling moment, kg-m
M_y	pitching moment, kg-m
M_z	yawing moment, kg-m
$(M_1/I)_{y, z}$	angular acceleration about the y- or z-axis due to aerodynamic forces, rad/sec ²
$(M_2/I)_x$	angular acceleration about the x-axis due to the engine deflection, rad/sec ²
$(M_2/I)_{y, z}$	angular acceleration about the y- or z-axis due to engine deflection, rad/sec ²
n	number of engines

DEFINITION OF SYMBOLS (Cont'd)

<u>Symbol</u>	<u>Definition</u>
$[\partial(M_e/I)_{y,z}/\partial\beta_{y,z}]_{\beta=0}$	gradient through $\beta_{y,z} = 0^\circ$ of angular acceleration about the y- or z-axis due to the deflection of one control engine in the pitch (xz) or yaw (xy) plane, $(\text{rad/sec}^2)/\text{deg } \beta_{y,z}$
$[\partial(M_e/I)_x/\partial\beta_{y,z}]_{\beta=0}$	gradient through $\beta_{y,z} = 0^\circ$ of angular acceleration about the x-axis due to the deflection of the control engine in the yaw (xy) or pitch (xz) plane, $(\text{rad/sec}^2)/\text{deg } \beta_{y,z}$
$[\partial(Y_2, Z_2/m)/\partial\beta_{y,z}]_{\beta=0}$	gradient through $\beta_{y,z} = 0^\circ$ of normal linear acceleration due to the deflection of one control engine in the yaw (xy) or pitch (xz) plane, $(\text{m/sec}^2)/\text{deg } \beta_{y,z}$
q	dynamic pressure, $\rho V^2/2$, kg/m^2
S	reference area, $\pi D^2/4$, m^2
V , (\vec{V})	velocity of missile or free-stream velocity vector, m/sec
x, y, z	coordinates of missile fixed coordinate system (see Figure A-1)
X	aerodynamic axial force, $C_x qS$, kg
Y_1	aerodynamic side force, $C_y qS$ or $\tau C_{y_\tau} qS$, kg
Y_1/m	sideward acceleration due to sideslip angle τ , m/sec^2
Y_1'/m	$\partial(Y_1/m)/\partial\tau$: gradient through $\tau = 0^\circ$ of sideward acceleration due to aerodynamic side forces, $(\text{m/sec}^2)/\text{deg } \tau$
Y_2/m	sideward acceleration due to the deflection of one control engine in the yaw (xy) plane, m/sec^2

DEFINITION OF SYMBOLS (Cont'd)

<u>Symbol</u>	<u>Definition</u>
Y'_2/m	$\partial(Y_2/m)/\partial\beta_y$: gradient through $\beta_y = 0^\circ$ of the sideward acceleration due to the deflection of one control engine in the yaw (xy) plane, $(m/sec^2)/deg \beta_y$
Z_1	aerodynamic normal force, $C_z qS$ or $\alpha C_{z\alpha} qS$, kg
Z_1/m	normal acceleration due to angle of attack, α , m/sec^2
Z'_1/m	$\partial(Z_1/m)/\partial\alpha$: gradient through $\alpha = 0^\circ$ of normal acceleration due to aerodynamic normal forces, $(m/sec^2)/deg \alpha$
Z_2/m	normal acceleration due to the deflection of one control engine in the pitch (xz) plane, m/sec^2
Z'_2/m	$\partial(Z_2/m)/\partial\beta_z$: gradient through $\beta_z = 0^\circ$ of the normal acceleration due to the deflection of one control engine in the pitch (xz) plane, $(m/sec^2)/deg \beta_z$
α	angle of attack, degree or radian
β_z	angle of engine deflection measured between projection of engine axis on xz-plane and x-axis (produces force parallel to the z-axis), degree or radian
β_y	angle of engine deflection measured between projection of engine axis on xy-plane and x-axis (produces force parallel to the y-axis), degree or radian
γ_1	cant angle of the inboard engines, degree or radian
γ_0	cant angle of the outboard engines, i.e., angle between nozzle axis of engine at $\beta_y = \beta_z = 0$ and the x-axis, degree or radian

DEFINITION OF SYMBOLS (Cont'd)

<u>Symbol</u>	<u>Definition</u>
λ_1	angle inscribed by the missile longitudinal axis and a line through the inboard engine pivot point and the missile center of gravity (optimum cant angle of inboard engine), degree or radian
λ_0	angle inscribed by the missile longitudinal axis and a line through the outboard engine gimbal point and the missile center of gravity (optimum cant angle of outboard engine), degree or radian
τ	angle of sideslip, degree or radian
φ	angle of roll, degree or radian

Superscripts

\circ	denotes quantity in degrees or per degree
\circ	denotes quantity in radians or per radian
'	derivative with respect to a normalized angle evaluated at zero angle

Subscripts

1	denotes quantity resultant of aerodynamic forces
2	denotes quantity resultant of engine deflection

NASA-GEORGE C. MARSHALL SPACE FLIGHT CENTER

TECHNICAL MEMORANDUM X-53296

CONTROL FACTORS FOR
APOLLO-SATURN 201 VEHICLE

By

Billy W. Nunley

SUMMARY

This report presents the control factor data to be used for Apollo-Saturn 201 vehicle control studies. Included are angular velocities, linear velocities, angular accelerations, and linear accelerations due to engine and aerodynamic forces. Also included are three-sigma variations of the more important control factors for the standard eight-engine case; i.e., no engine-out conditions were studied.

I. INTRODUCTION

The multiple-engine arrangement of the Saturn IB vehicle introduces a complexity in the engine control factor calculation and presentation. This is a result of off-axis, canted engines. A body-fixed coordinate system with its origin at the longitudinal location of the vehicle center of gravity is employed. To clearly define the control factors, a system of signs, symbols, and equations (discussed in Appendix A) was established by the Aerodynamic Design Branch [1].

II. VEHICLE DESCRIPTION AND MISSION

A schematic of the Apollo-Saturn 201 is shown in Figure 1. The vehicle has eight 53-square-foot fins to improve the static aerodynamic stability. The first stage flight configuration consists of S-IB first stage, S-IVB second stage, instrument unit (IU), lunar excursion module (LEM) adapter, service module (SM), command module (CM), and launch escape system (LES). The first stage reference diameter is 257 inches.

The S-IB stage propulsion system consists of eight Rocketdyne H-1, 200 thousand pound thrust engines. The four inboard engines, located on a 32-inch radius, have a fixed cant of 3° to the vehicle longitudinal axis. The four control (outboard) engines, located on a 95-inch radius, are free to gimbal in a ±8° square pattern and have a fixed cant of 6° to the vehicle longitudinal axis.

The S-IVB stage propulsion system consists of one Rocketdyne J-2, 200 thousand pound thrust engine, which is located on the vehicle longitudinal axis.

The primary mission of SA-201 is to demonstrate the compatibility and performance of the launch vehicle/spacecraft in preparation for manned orbital missions. Other missions of the SA-201 are the reentry and recovery of the command module.

III. AERODYNAMICS, MASS, AND TRAJECTORY DATA

The aerodynamic drag used in trajectory calculations is published in Reference 2. The normal force coefficient gradients and centers of pressure based on the most recent analysis of all available experimental data, will be published in the near future. The variations from the nominal values applied to the aerodynamic data were ±10 per cent on drag coefficient, ±6 per cent on normal force gradient, and ±0.2 calibers on center of pressure.

The mass data used are published in Reference 3. The center of gravity, pitch and yaw moment of inertia, and roll moment of inertia are presented in Figures 2 through 4, respectively. The variations applied to the mass data are 10 inches on center of gravity, 5 per cent on pitch moment of inertia, and 5 per cent on yaw moment of inertia.

The nominal trajectory data, tabulated in Table I, are unpublished working data obtained from the Applied Guidance and Flight Mechanics Branch. The trajectories employed with variations in thrust, specific impulse propellant loading, axial force, and incorporating winds are published in Reference 4.

IV. DATA PRESENTATION AND DISCUSSION

This report presents the standard control factor data and three-sigma variation analysis for the standard eight-engine case. The variations of C_1 , C_2 , Z'_1/m , and Z'_2/m and corresponding ratios C_1/C_2 , $(Z'_1/m)/(Z'_2/m)$, $C_1/(Z'_1/m)$, and $C_2(Z'_2/m)$ are presented as a function of time.

- Symbols and sign convention used are discussed in Appendix A. Control factors, especially the quantities involving engine forces (see Figures 8, 11, and 13), are discussed in detail in Reference 1.

The vehicle stability margin is presented in Figure 5 as a function of time. The maximum stability and instability have magnitudes of -0.04 and 1.63 at flight times of 62 and 140 seconds, respectively. The stable region occurs near Mach 1.0 since the influence of the fins is a maximum. Maximum dynamic pressure occurs approximately 76.9 seconds after liftoff ($M = 1.46$).

Figure 6 presents the engine cant angles versus time. The four inboard engines have a fixed cant angle of 3° to the vehicle longitudinal axis; the four outboard engines are canted 6° to the vehicle axis. Also presented are the optimum cant angle for the outboard and inboard engines.

The gradients of angular accelerations due to aerodynamic forces versus time are presented in Figure 7. These data are linearized through zero angle of attack and should not be used at angles of attack greater than 6° . Since the vehicle is symmetrical, these data are applicable to accelerations about both the pitch and yaw axes. The maximum stabilizing and overturning accelerations occur at $t = 61$ and 87 seconds, respectively. The vehicle is stable in the region near Mach 1.0, $t = 61$ to 62 seconds.

The gradients of angular acceleration due to engine forces are presented in Figure 8. The presentation scheme is discussed in Reference 1. A_0 and A_1 are bias accelerations and B^0 is linearized through $\beta_{y,z} = 0^\circ$. A_0 , A_1 , and B^0 represent the data for one engine; the total accelerations are obtained by the algebraic summation scheme shown in the accompanying table. This scheme includes summing the components of all engines operating.

The ratio of aerodynamic and engine angular accelerations is shown in Figure 9. These data are for four control engines and give quasi-steady state β/α for control.

Three-sigma variations of C_1 , C_2 , and C_1/C_2 for selected time points are shown in Figure 10. The number of boxes was restricted to maintain clarity; data at other time points are tabulated in Tables II, III, and IV. CAUTION SHOULD BE EXERCISED IN USING THE TABULATED DATA. (SEE APPENDIX B FOR A DISCUSSION OF THEIR USE). The boxes represent the range of possible C_1-C_2 combinations with three-sigma limitation. The legend gives information on the box boundaries.

Gradients of angular accelerations in roll due to engine forces are presented versus flight time in Figure 11. These data, linearized through $\beta_{y,z} = 0^\circ$, represent the data for one engine. Total accelerations are obtained by the algebraic summation scheme shown in the accompanying table.

Figure 12 shows the gradients of linear accelerations due to aerodynamic forces as a function of flight time. These data are linearized through zero angle of attack and are valid only to $\alpha = \pm 6^\circ$ since the aerodynamic data are nonlinear with respect to angle of attack. These data are applicable to accelerations in the Z (normal) and Y (sideward) directions.

Gradient of linear accelerations due to engine forces is shown in Figure 13 versus flight time. J_0 and J_1 are bias accelerations, and K^0 represents the data for one engine. The total accelerations are obtained by the algebraic summation scheme shown in the accompanying table.

Figure 14 presents the resultant axial acceleration due to aerodynamic and engine forces. The dip at 142 seconds is due to inboard engine cutoff.

Angular velocities (damping factor) due to aerodynamic forces are shown in Figure 15. The contribution of the fuel forces has not been calculated.

TABLE I
Nominal Trajectory Data

t sec	M	q kg/m ²	V m/sec	Alt km
1.0	0.007	0.31	2.3	0.001
5.0	0.035	8.85	12.1	0.003
10.0	0.075	40.40	26.0	0.123
15.0	0.121	102.01	41.7	0.292
20.0	0.172	200.94	59.1	0.544
25.0	0.229	343.55	78.6	0.887
30.0	0.293	533.78	100.1	1.333
35.0	0.364	772.74	123.7	1.890
40.0	0.444	1057.55	149.8	2.571
45.0	0.533	1381.31	178.4	3.384
50.0	0.633	1733.36	209.9	4.341
55.0	0.747	2098.09	244.6	5.451
60.0	0.877	2450.70	282.4	6.721
65.0	1.020	2728.18	321.4	8.155
70.0	1.180	2917.14	362.7	9.745
75.0	1.369	3023.07	408.9	11.495
80.0	1.585	2997.81	461.3	13.414
85.0	1.820	2798.62	520.7	15.511
90.0	2.054	2432.78	587.9	17.797
95.0	2.278	1991.25	663.4	20.282
100.0	2.526	1599.64	747.1	22.977
105.0	2.802	1257.15	829.3	25.887
110.0	3.101	963.02	940.1	29.021
115.0	3.407	713.08	1049.8	32.383
120.0	3.725	514.40	1168.7	35.981
125.0	4.054	362.91	1297.5	39.822
130.0	4.406	252.25	1436.8	43.913
135.0	4.806	174.05	1587.3	48.266
140.0	5.354	121.43	1749.2	52.891
*141.0	5.449	111.36	1773.2	53.852
**148.65	5.887	49.05	1841.45	61.228

*Inboard Engine Cutoff

**Outboard Engine Cutoff

TABLE II
 C_1 Variations

t sec	σ Level	MIN	STD	MAX	TOL	BIA
		$(\text{Rad}/\text{Sec}^2)/\text{Deg } \alpha$			\pm %	%
0.1	3	0.00000	0.00000	0.00000	59.7	0.02
10.0		0.00001	0.00004	0.00006	69.2	0.02
20.0		0.00004	0.00017	0.00030	73.8	0.02
30.0		0.00013	0.00046	0.00080	72.6	0.02
40.0		0.00025	0.00091	0.00157	73.1	0.02
50.0		0.00020	0.00131	0.00242	84.8	0.00
60.0		-0.00145	0.00033	0.00212	535.7	0.77
70.0		-0.00014	0.00204	0.00420	106.2	-0.63
80.0		0.00239	0.00536	0.00784	50.8	-4.61
90.0		0.00611	0.00793	0.00968	22.6	-0.45
100.0		0.00435	0.00560	0.00679	21.8	-0.60
110.0		0.00218	0.00303	0.00384	27.3	-0.65
120.0		0.00055	0.00110	0.00174	53.9	3.49
130.0		0.00029	0.00059	0.00095	54.7	3.71
139.99		-0.00553	0.00094	0.00741	687.7	-0.05

TABLE III

 C_2 Variation

t sec	σ Level	MIN	STD	MAX	TOL	BIA
		(Rad/Sec ²)/Deg β			\pm %	%
0.1	3	0.01266	0.01333	0.01406	5.26	0.24
10.0		0.01271	0.01340	0.01415	5.37	0.23
20.0		0.01280	0.01349	0.01425	5.38	0.23
30.0		0.01292	0.01362	0.01439	5.39	0.23
40.0		0.01314	0.01386	0.01464	5.39	0.23
50.0		0.01346	0.01419	0.01499	5.40	0.23
60.0		0.01389	0.01465	0.01547	5.40	0.23
70.0		0.01410	0.01523	0.01642	7.62	0.16
80.0		0.01518	0.01600	0.01690	5.37	0.23
90.0		0.01615	0.01702	0.01797	5.34	0.24
100.0		0.01746	0.01839	0.01941	5.31	0.24
110.0		0.01933	0.02036	0.02149	5.29	0.24
120.0		0.02221	0.02339	0.02468	5.28	0.24
130.0		0.02674	0.02846	0.03029	6.23	0.20
139.99		0.03391	0.03799	0.04217	10.88	0.12

TABLE IV C_1/C_2 Variations

t sec	σ Level	MIN	STD	MAX	TOL	BIA
		β/α for Pitch-Yaw Control			$\pm \%$	%
0.1	3	0.00001	0.00003	0.00005	59.7	0.00
10.0		0.00083	0.00263	0.00454	69.1	0.00
20.0		0.00333	0.01260	0.02199	73.7	0.00
30.0		0.00930	0.03391	0.05851	72.6	0.00
40.0		0.01770	0.06579	0.11387	73.1	0.00
50.0		0.01401	0.09264	0.17125	84.9	-0.01
60.0		-0.09900	0.02277	0.14488	535.6	0.77
70.0		-0.01242	0.13402	0.27878	108.6	-0.62
80.0		0.15089	0.33503	0.48772	50.3	-4.69
90.0		0.35896	0.46593	0.56818	22.5	-0.51
100.0		0.23602	0.30457	0.36911	21.8	-0.66
110.0		0.10691	0.14886	0.18873	27.5	-0.70
120.0		0.02328	0.04714	0.07426	54.1	3.46
130.0		0.01027	0.02097	0.03320	54.7	3.69
139.99		-0.14360	0.02478	0.19314	679.5	-0.05

TABLE V

 Z_1/m Variations

t sec	σ Level	MIN	STD	MAX	TOL	BIA
		$(m/sec^2)/Deg \alpha$			$\pm \%$	%
0.1	3	0.00002	0.00002	0.00003	16.8	0.00
10.0		0.00206	0.00248	0.00290	16.9	0.00
20.0		0.01127	0.01328	0.01530	15.2	0.01
30.0		0.03260	0.03744	0.04229	12.9	0.01
40.0		0.07045	0.07913	0.08783	11.0	0.00
50.0		0.12696	0.14133	0.15519	10.0	-0.18
60.0		0.20016	0.23179	0.25993	12.9	-0.75
70.0		0.26079	0.29038	0.31255	8.9	-1.28
80.0		0.25729	0.29330	0.31926	10.6	-1.71
90.0		0.19471	0.22784	0.25902	14.1	-0.43
100.0		0.13012	0.15343	0.17421	14.4	-0.82
110.0		0.07854	0.09839	0.11588	19.0	-1.20
120.0		0.04150	0.05654	0.07070	25.8	-0.78
130.0		0.02068	0.02967	0.03813	29.4	-0.91
139.99		-0.11994	0.02015	0.16022	695.1	-0.09

TABLE VI
 Z_2/m Variations

t sec	σ Level	MIN	STD	MAX	TOL	BIA
		$(m/sec^2)/Deg \beta$			\pm %	%
0.1	3	0.10476	0.10539	0.10602	0.6	0.00
10.0		0.11077	0.11205	0.11332	1.1	0.00
20.0		0.11777	0.11915	0.12053	1.2	0.00
30.0		0.12563	0.12715	0.12867	1.2	0.00
40.0		0.13486	0.13655	0.13824	1.2	0.00
50.0		0.14558	0.14745	0.14933	1.3	0.00
60.0		0.15778	0.15985	0.16192	1.3	0.00
70.0		0.16415	0.17378	0.18341	5.5	0.00
80.0		0.18688	0.18926	0.19164	1.3	0.00
90.0		0.20418	0.20667	0.20916	1.2	0.00
100.0		0.22327	0.22592	0.22852	1.2	0.00
110.0		0.24509	0.24793	0.25077	1.1	0.00
120.0		0.27069	0.27383	0.27698	1.1	0.00
130.0		0.29596	0.30533	0.31470	3.1	0.00
139.99		0.30609	0.34336	0.38063	10.85	0.00

TABLE VII
 $(z_1/m)/(z_2/m)$ Variations

t sec	σ Level	MIN STD MAX			TOL <u>± %</u>	BIA %
		β/α for Normal Translation Control				
0.1	3	0.00018	0.00021	0.00025	16.8	0.00
10.0		0.01852	0.02210	0.02568	16.2	0.00
20.0		0.09541	0.11147	0.12754	14.4	0.01
30.0		0.25871	0.29445	0.33024	12.1	0.01
40.0		0.52080	0.57949	0.63823	10.1	0.00
50.0		0.86882	0.95848	1.04430	9.2	-0.20
60.0		1.26520	1.45000	1.61110	11.9	-0.81
70.0		1.46780	1.67090	1.83960	11.1	-1.03
80.0		1.35430	1.54960	1.69350	10.9	-1.66
90.0		0.93554	1.10240	1.26020	14.7	-0.42
100.0		0.57158	0.67920	0.77613	15.1	-0.79
110.0		0.31431	0.39686	0.47018	19.6	-1.16
120.0		0.15023	0.20645	0.25955	26.5	-0.76
130.0		0.06704	0.09718	0.12560	30.1	-0.89
139.99		-0.34447	0.05870	0.46176	686.8	-0.09

TABLE VIII
 $C_1/(Z_1/m)$ Variations

t sec	σ Level	MIN	STD	MAX	TOL	BIA
		$(\text{rad/sec}^2)/(\text{m/sec}^2)$				
0.1	3	0.00765	0.01788	0.02812	57.3	0.02
10.0		0.00475	0.01451	0.02428	67.3	0.02
20.0		0.00357	0.01286	0.02215	72.2	0.02
30.0		0.00352	0.01234	0.02115	71.4	0.02
40.0		0.00319	0.01152	0.01986	72.3	0.02
50.0		0.00144	0.00930	0.01717	84.5	0.02
60.0		-0.00625	0.00144	0.00916	535.5	1.29
70.0		-0.00035	0.00703	0.01437	104.7	-0.30
80.0		0.00868	0.01828	0.02673	49.4	-3.17
90.0		0.02816	0.03481	0.04147	19.1	0.02
100.0		0.03038	0.03651	0.04269	16.9	0.07
110.0		0.02497	0.03080	0.03668	19.0	0.07
120.0		0.01196	0.01950	0.02774	40.5	1.82
130.0		0.01111	0.02011	0.02969	46.2	1.44
139.99		0.04038	0.04672	0.05348	14.0	0.45

TABLE IX

 $C_2/(Z_2/m)$ Variations

t sec	σ Level	MIN	STD	MAX	TOL	BIA
		$(\text{rad/sec}^2)/(\text{m/sec}^2)$			$\pm \%$	%
0.1	3	0.12012	0.12646	0.13340	5.25	0.24
10.0		0.11361	0.11960	0.12617	5.25	0.24
20.0		0.10755	0.11323	0.11945	5.25	0.24
30.0		0.10176	0.10714	0.11303	5.26	0.24
40.0		0.09640	0.10148	0.10705	5.26	0.24
50.0		0.09142	0.09625	0.10153	5.25	0.24
60.0		0.08703	0.09162	0.09664	5.25	0.24
70.0		0.08329	0.08768	0.09249	5.24	0.24
80.0		0.08033	0.08455	0.08918	5.23	0.24
90.0		0.07825	0.08236	0.08686	5.22	0.24
100.0		0.07737	0.08141	0.08585	5.21	0.24
110.0		0.07805	0.08212	0.08658	5.19	0.24
120.0		0.08120	0.08541	0.09004	5.18	0.24
130.0		0.08860	0.09321	0.09827	5.18	0.24
139.99		0.10510	0.11065	0.11674	5.26	0.24

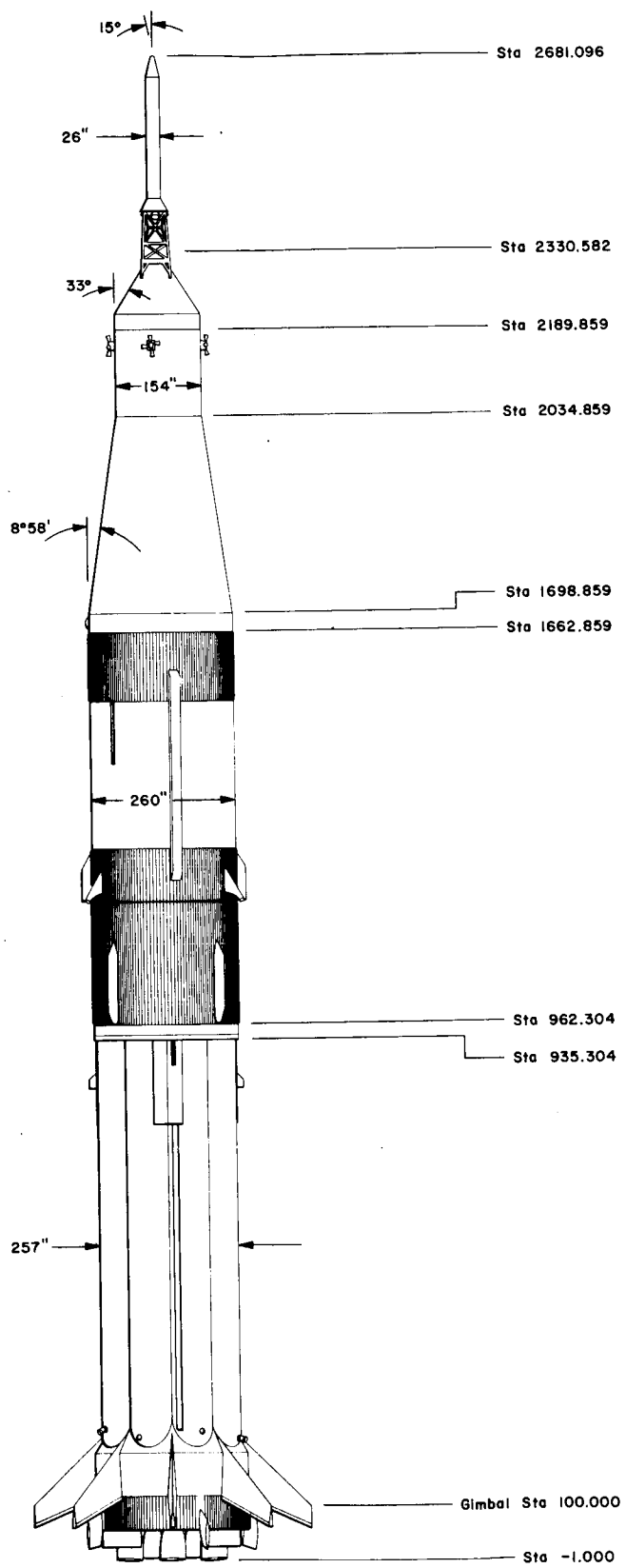


FIGURE 1 APOLLO-SATURN 201 VEHICLE CONFIGURATION

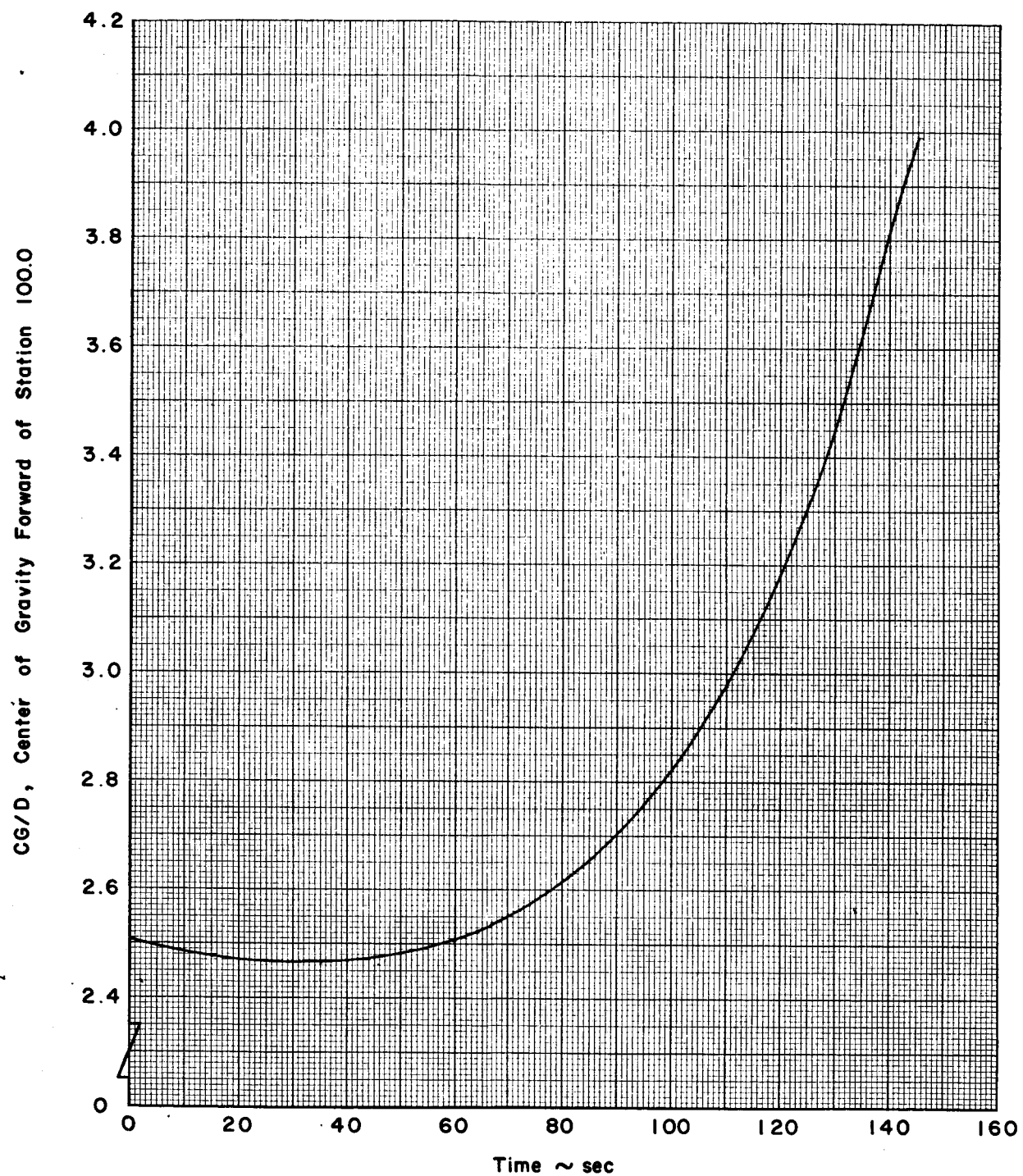


Figure 2 Variation of Center of Gravity with Flight Time

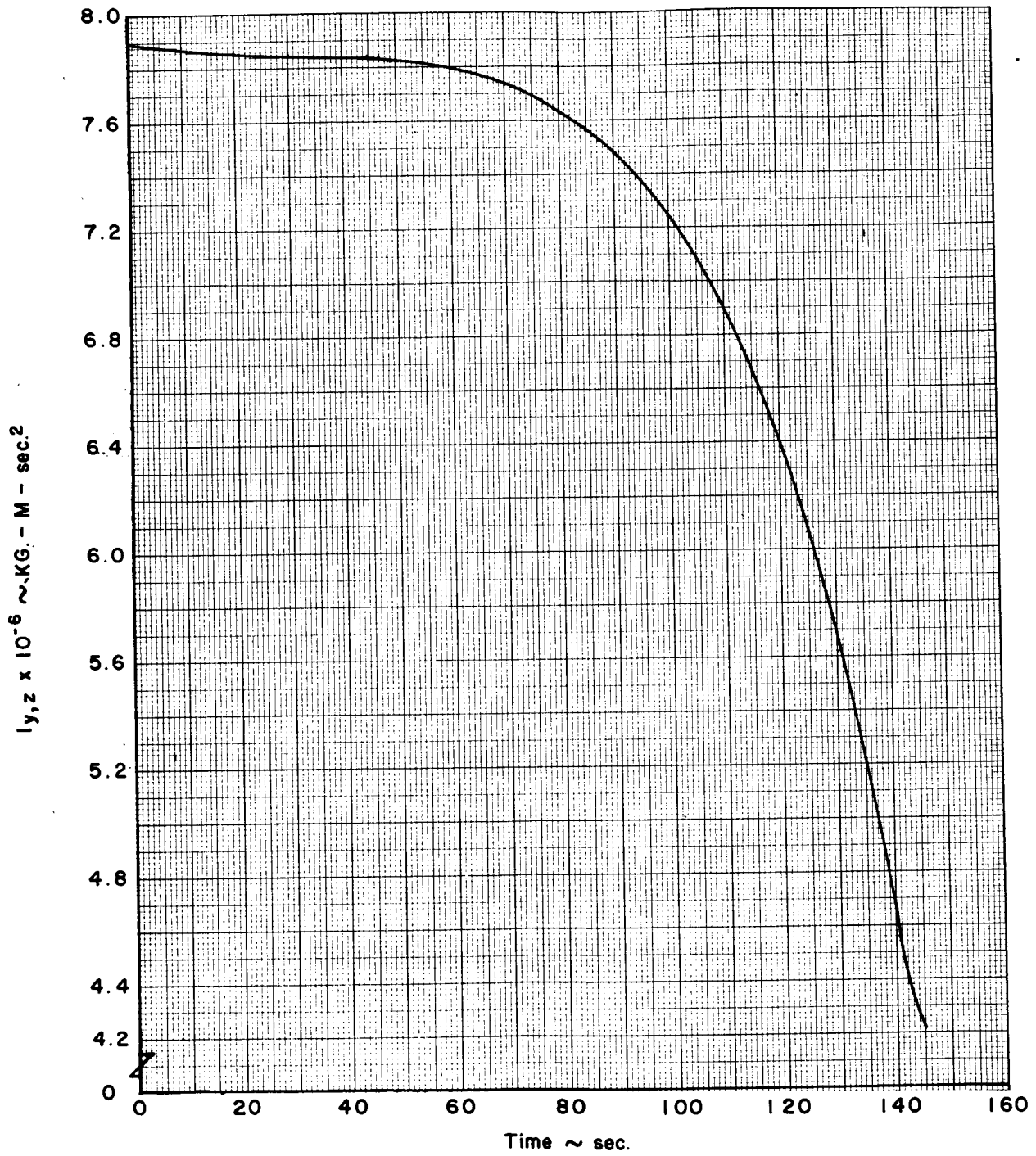
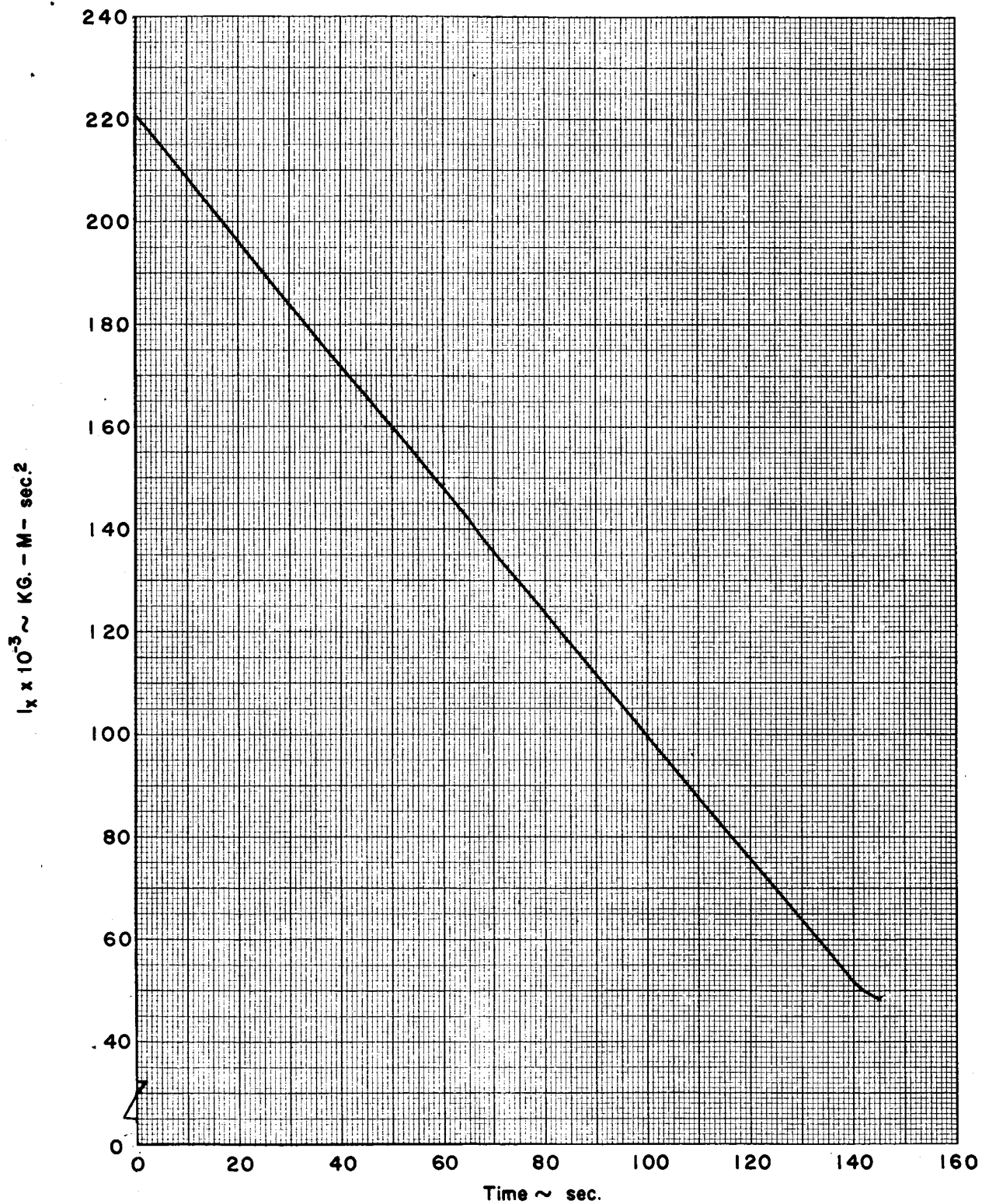


Figure 3 Variation of Pitch and Yaw Moment of Inertia vs Flight Time



**Figure 4 Variation of Roll Moment of Inertia
vs .Time**

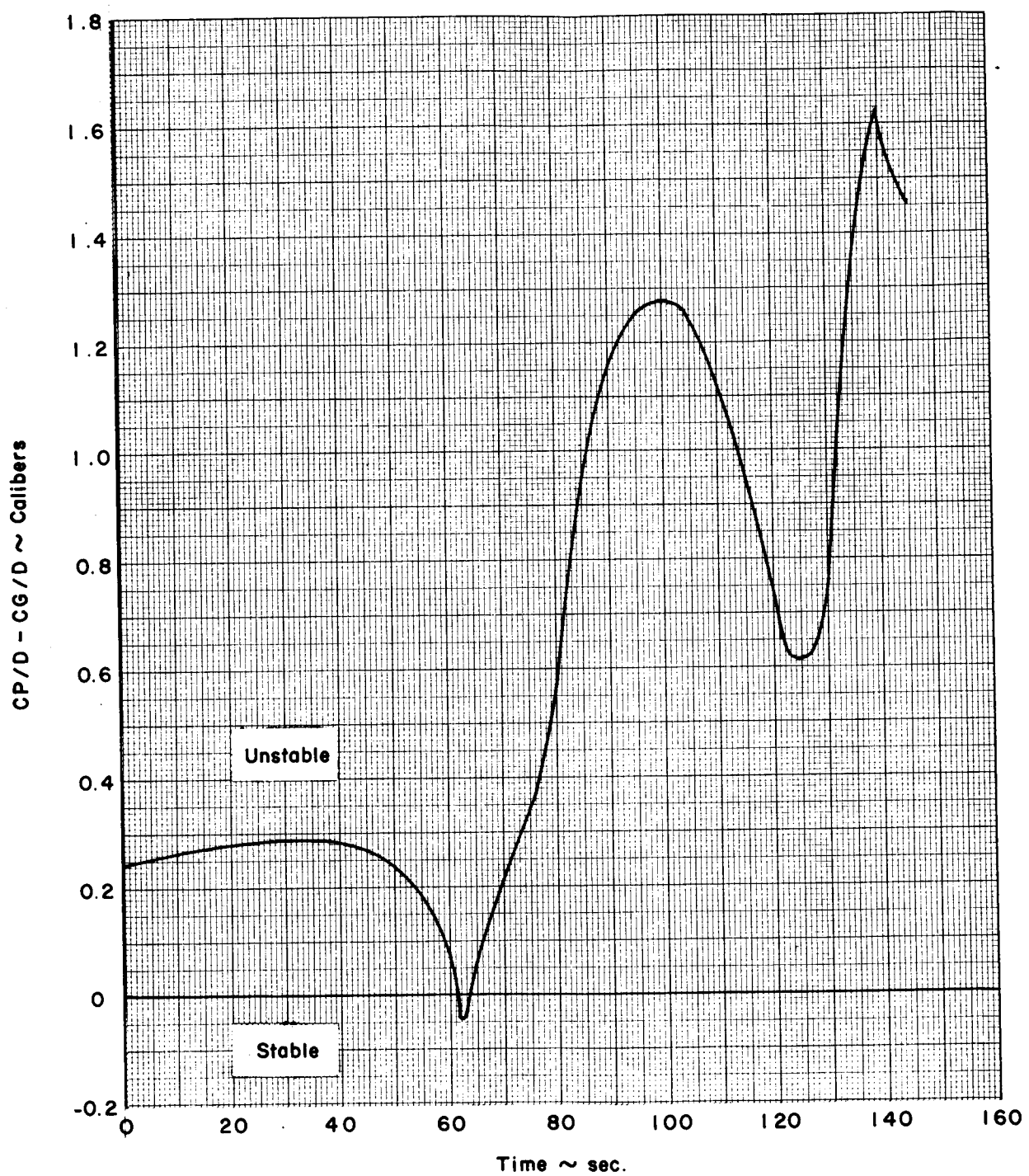


Figure 5 Variation of Stability Margin with Flight Time

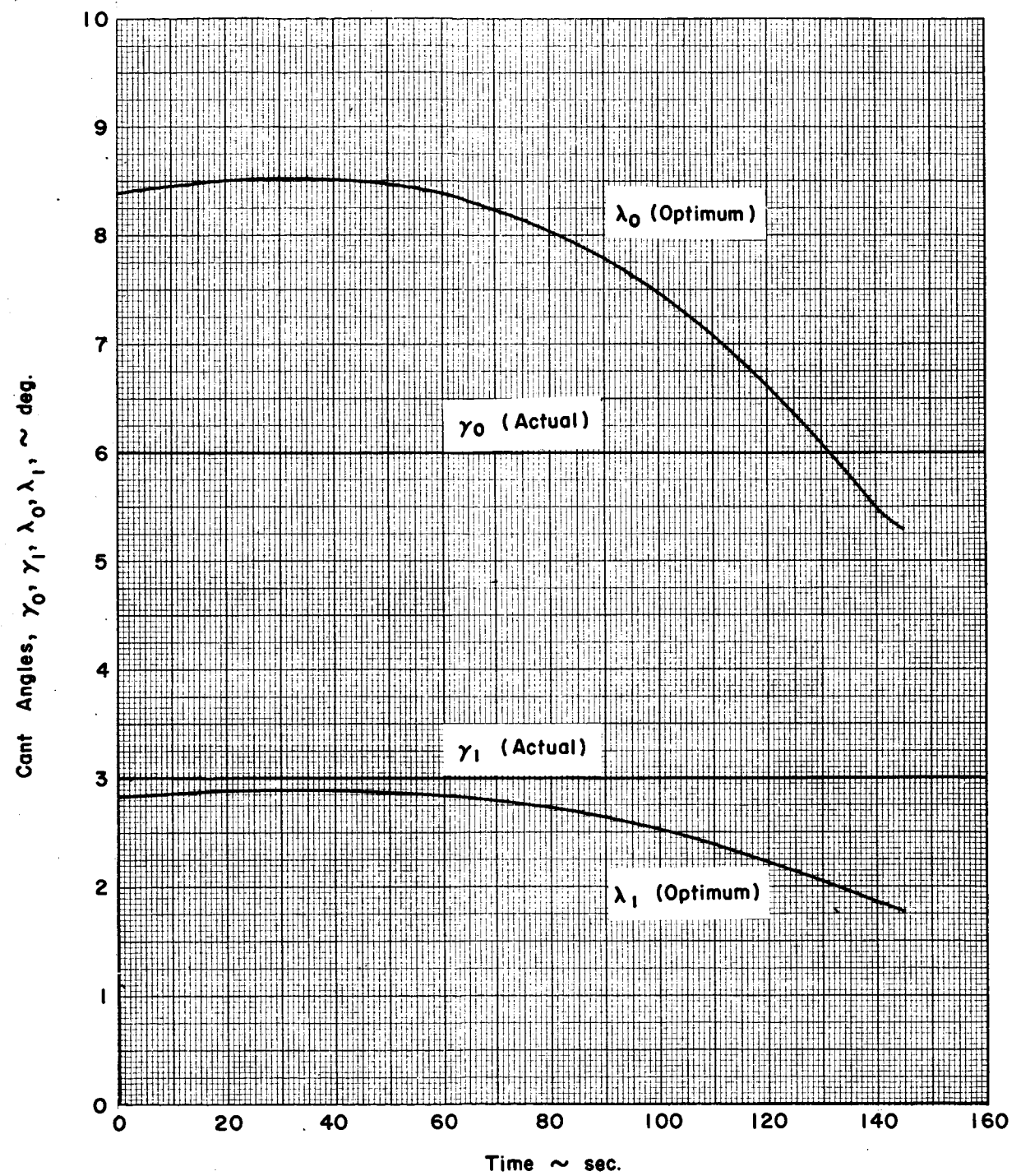


Figure 6 Cant Angle vs Time

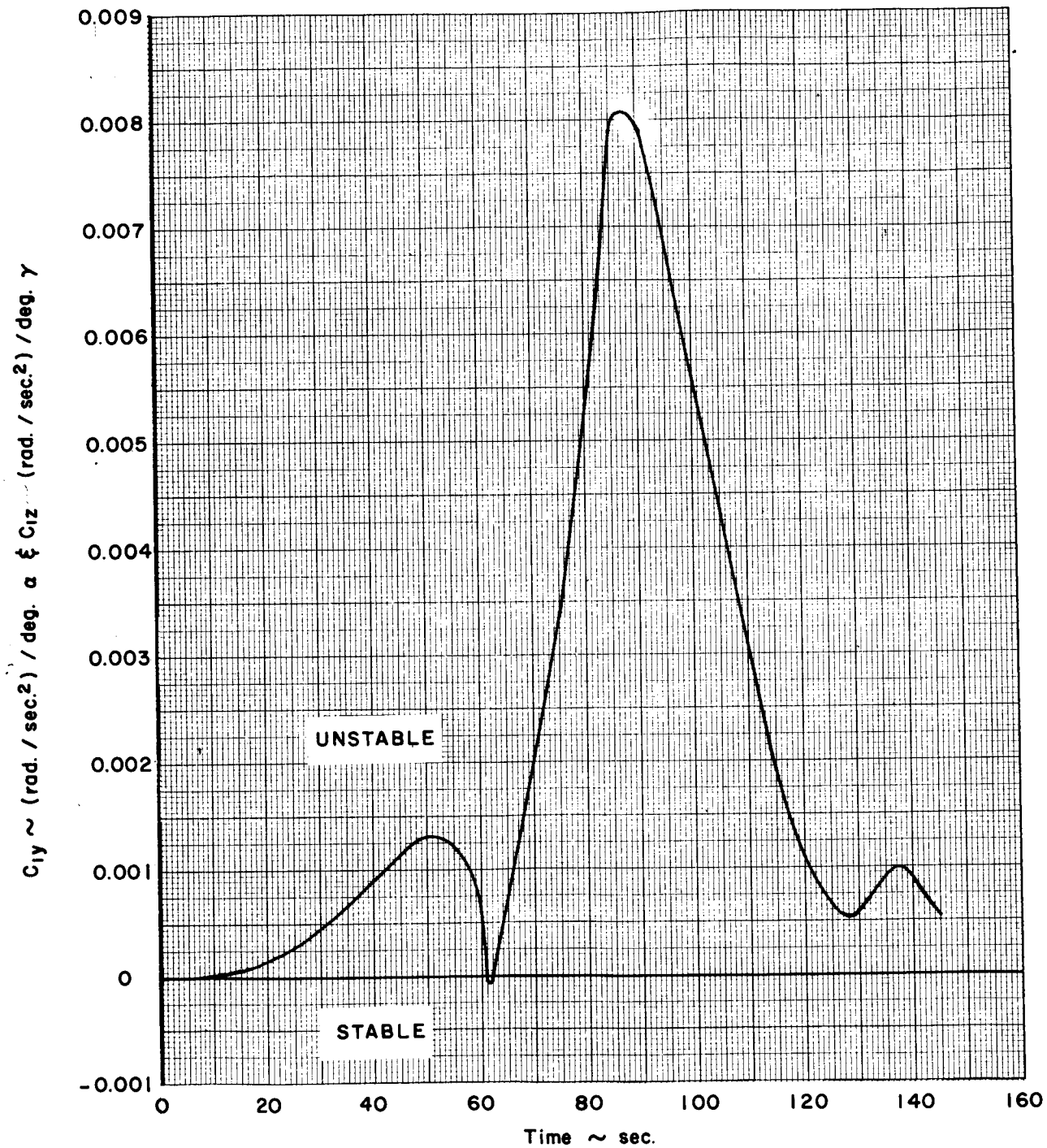
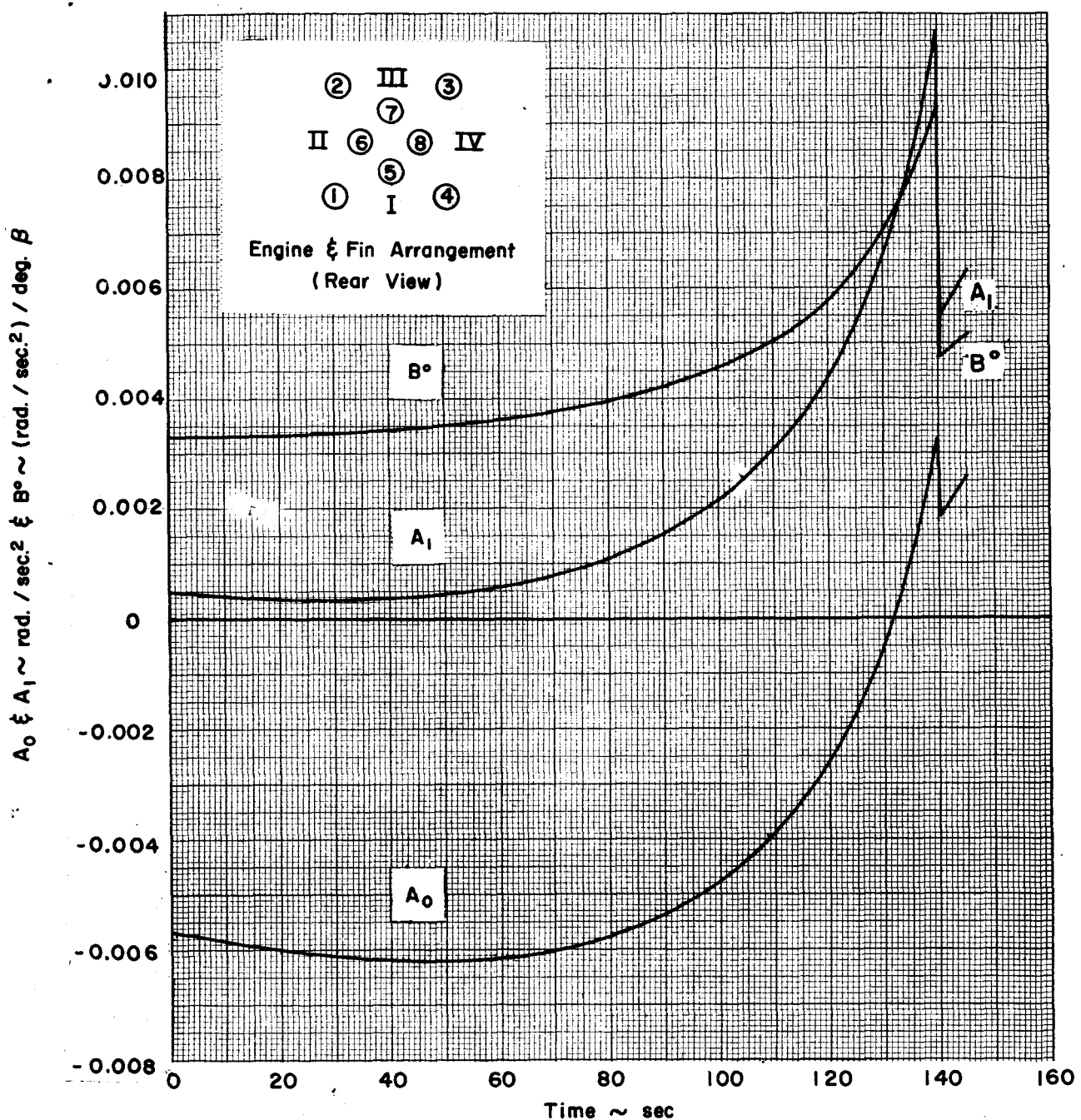


Figure 7 Variation of Angular Accelerations due to Aerodynamic Forces vs Time



	Eng. # 1	Eng. # 2	Eng. # 3	Eng. # 4	Eng. # 5	Eng. # 6	Eng. # 7	Eng. # 8
$(M_2/I)_y$	$-A_0 - B^o \beta_z^o$	$+A_0 - B^o \beta_z^o$	$+A_0 - B^o \beta_z^o$	$-A_0 - B^o \beta_z^o$	$-A_1$	0	$+A_1$	0
$(M_2/I)_z$	$-A_0 + B^o \beta_y^o$	$-A_0 + B^o \beta_y^o$	$+A_0 + B^o \beta_y^o$	$+A_0 + B^o \beta_y^o$	0	$-A_1$	0	$+A_1$

Figure 8 Variation of Angular Acceleration due to Engine Forces with Time

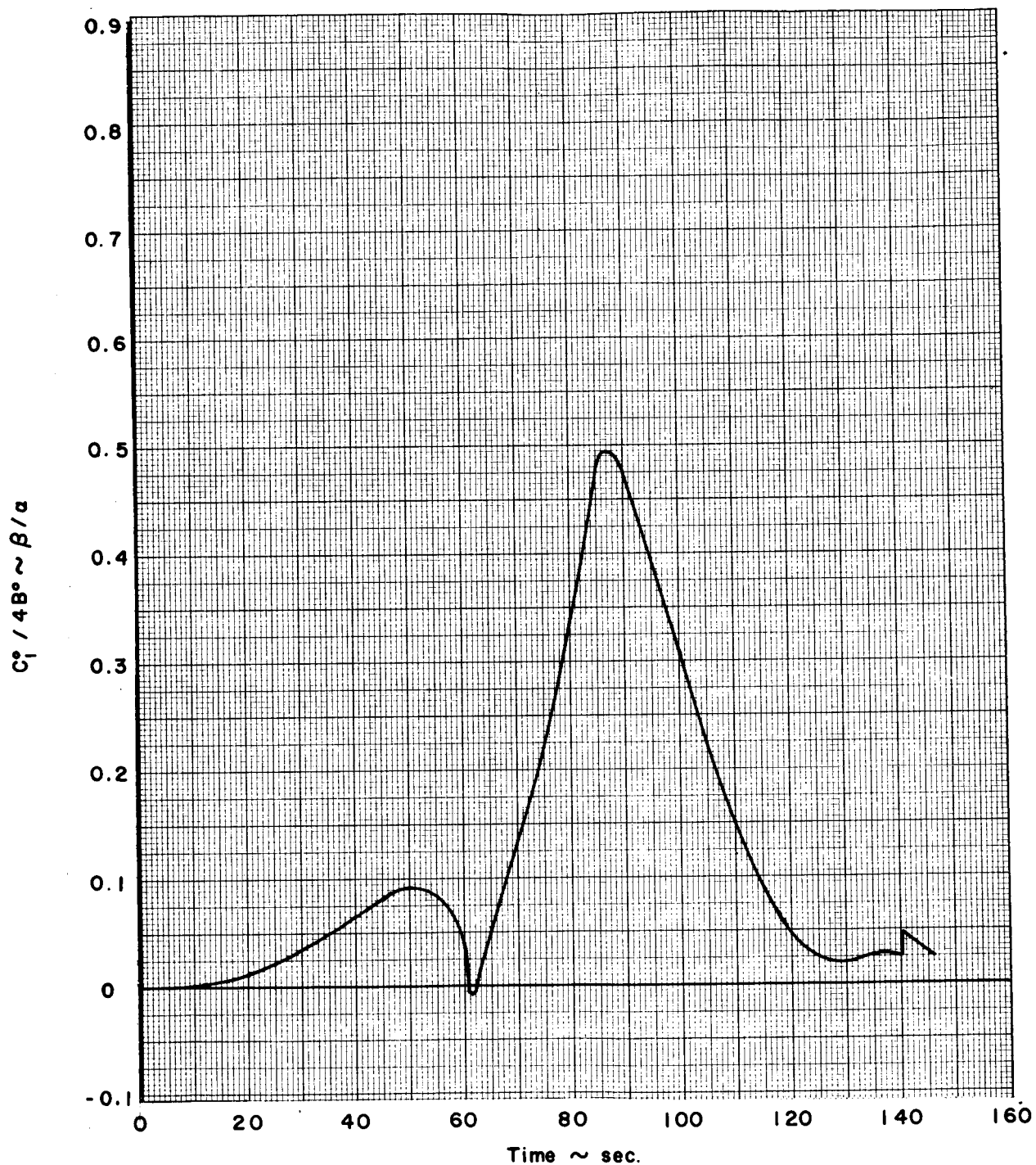


Figure 9 Variation of Ratio of Gradients of Angular Acceleration vs Time

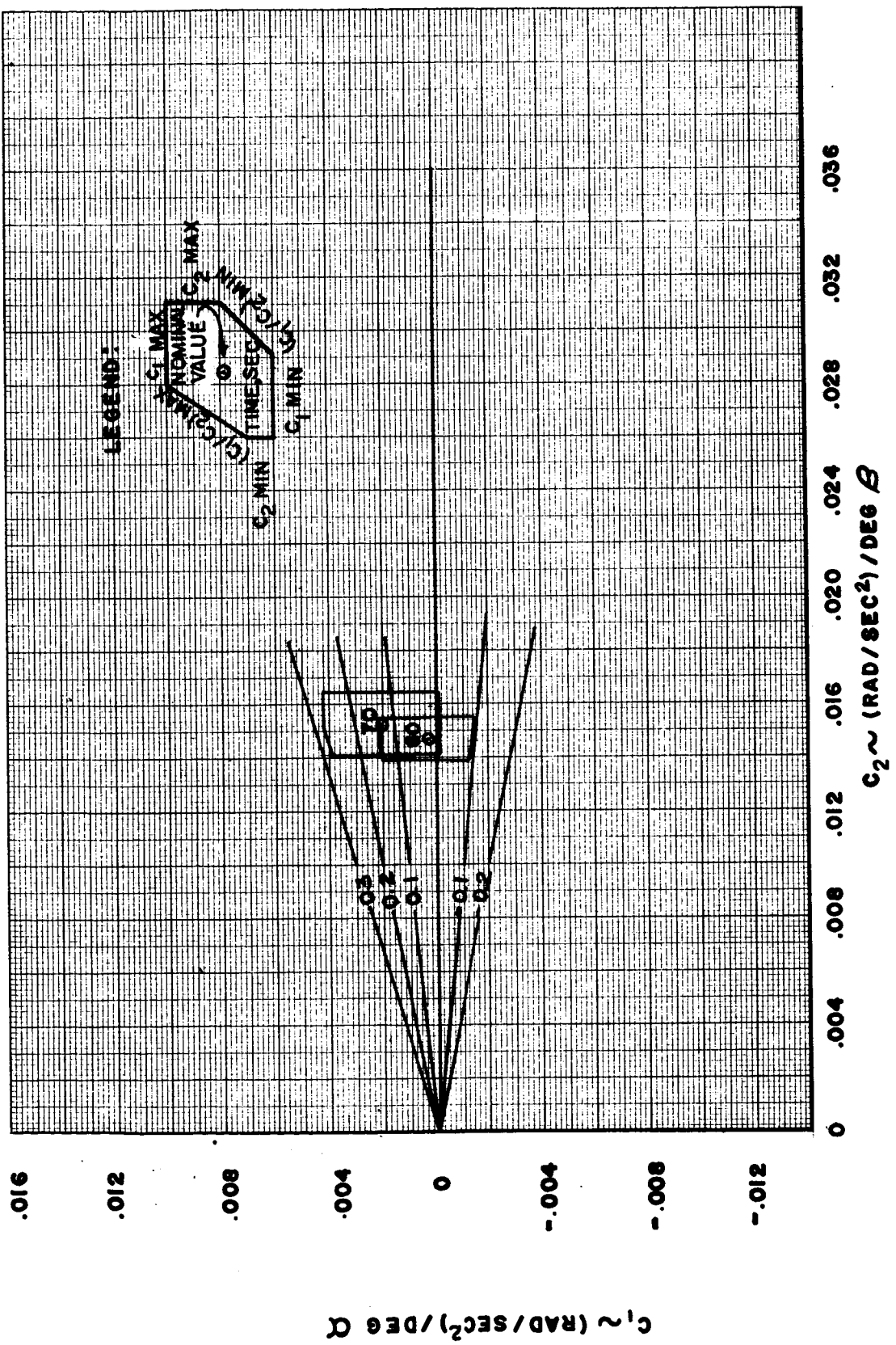


Figure 10 Three-Sigma Variations of C_1 , C_2 , and C_1/C_2

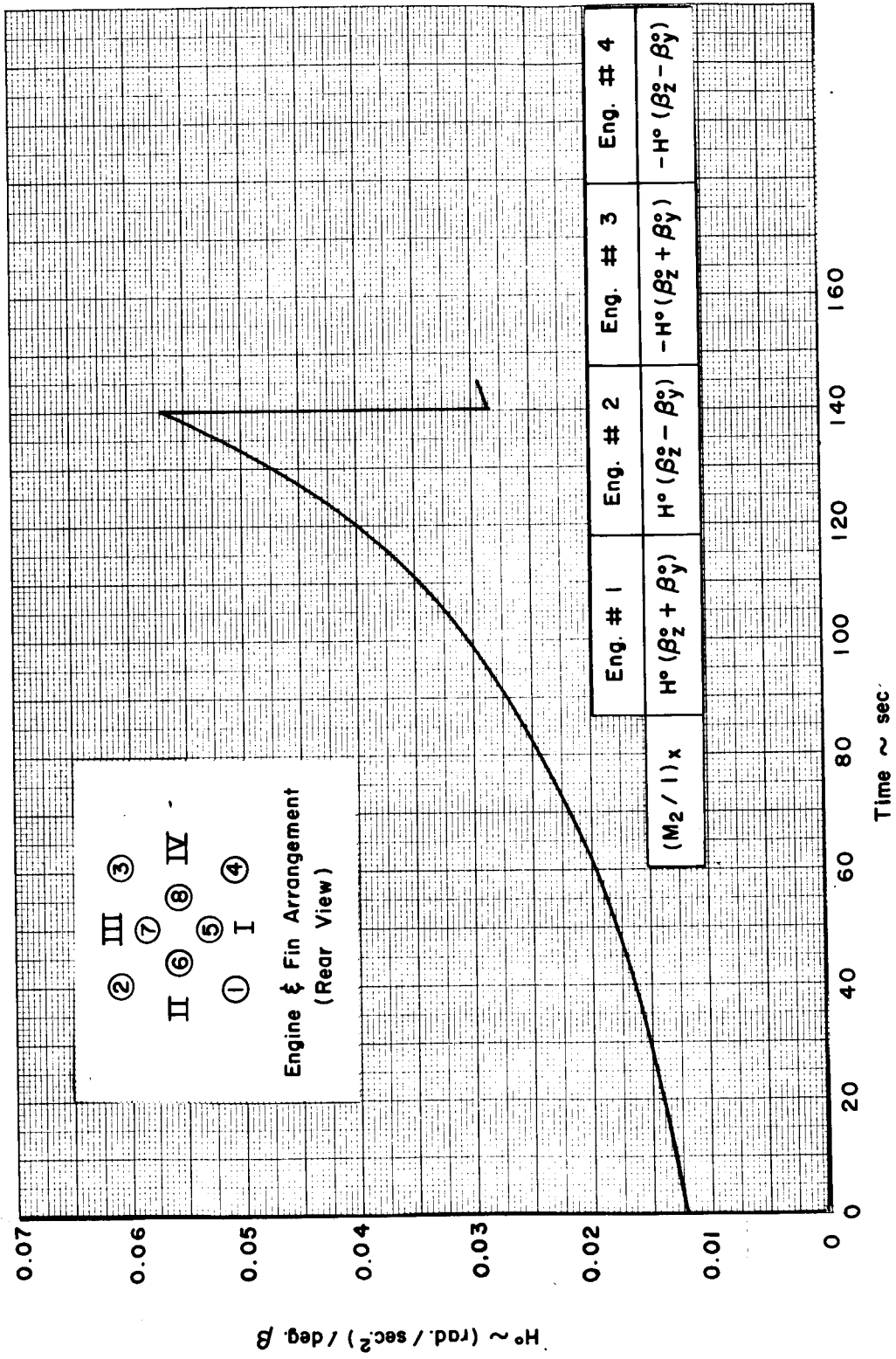


Figure 11 Variation of Angular Acceleration in Roll due to Engine Forces with Time

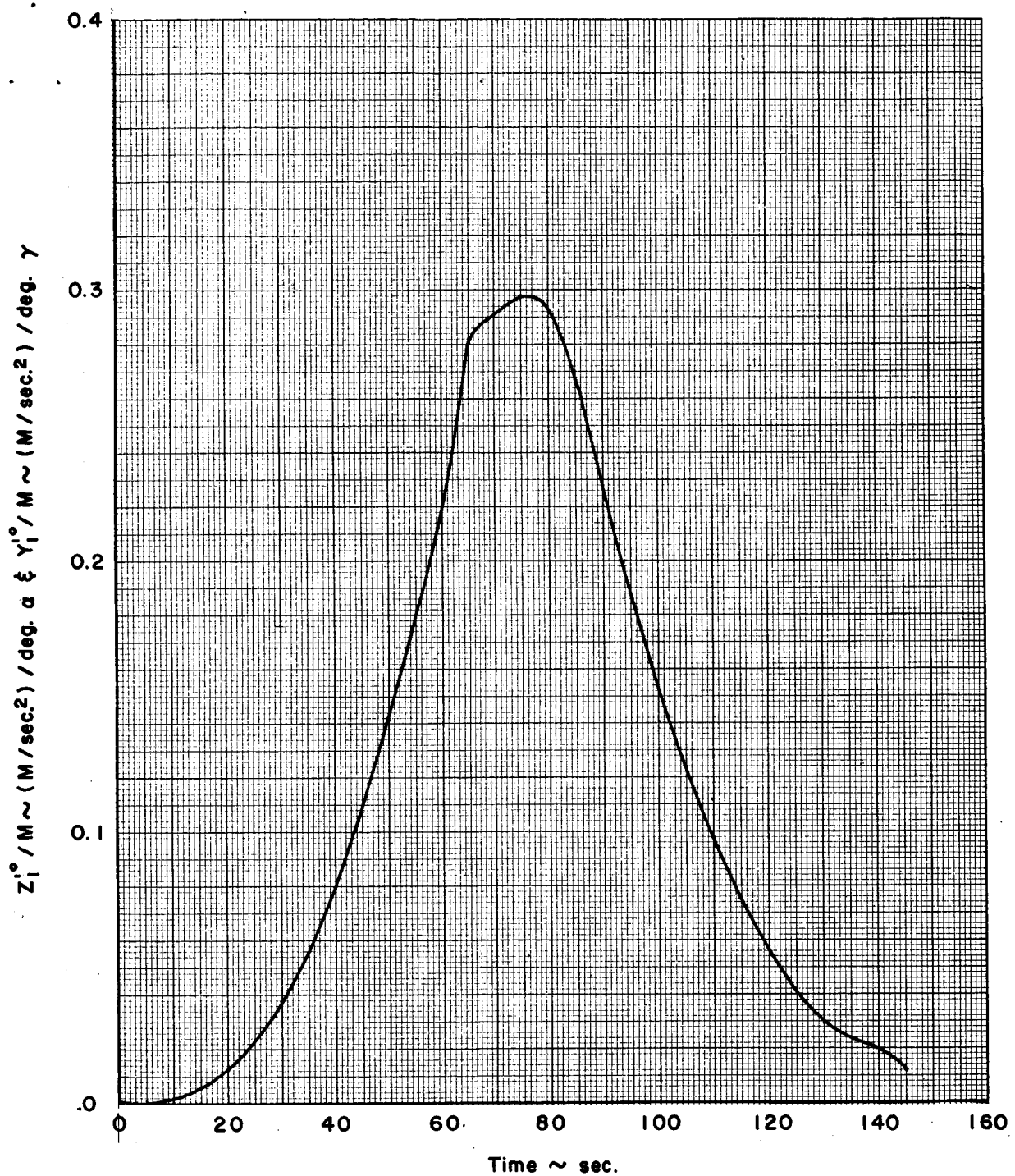
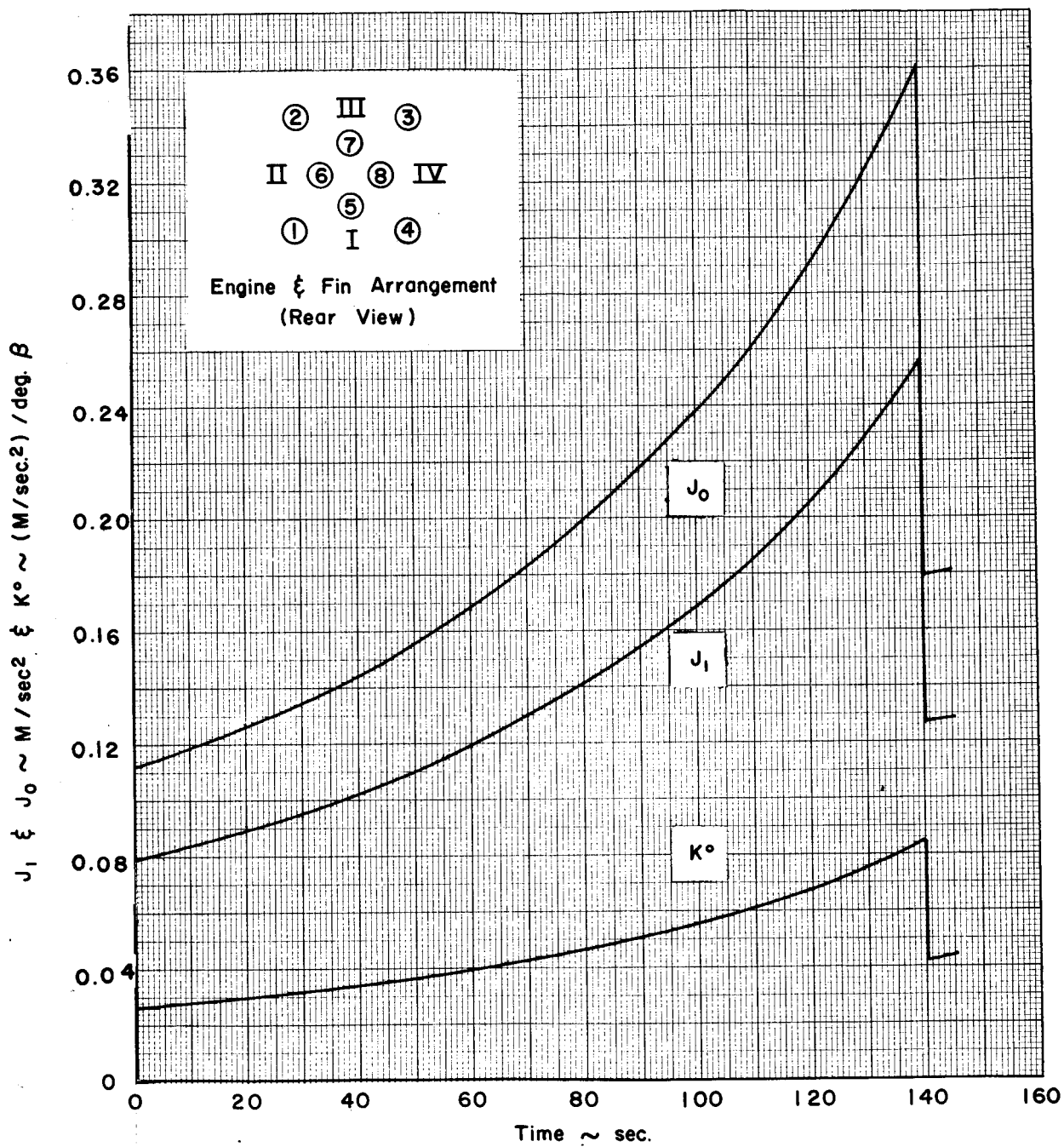


Figure 12 Variation of Linear Acceleration due to Aerodynamic Forces vs Time



	Eng. # 1	Eng. # 2	Eng. # 3	Eng. # 4	Eng. # 5	Eng. # 6	Eng. # 7	Eng. # 8
$Z_2 M$	$+J_0 + K^\circ \beta_z^\circ$	$-J_0 + K^\circ \beta_z^\circ$	$-J_0 + K^\circ \beta_z^\circ$	$+J_0 + K^\circ \beta_z^\circ$	$+J_1$	0	$-J_1$	0
$Y_2 M$	$-J_0 + K^\circ \beta_y^\circ$	$-J_0 + K^\circ \beta_y^\circ$	$+J_0 + K^\circ \beta_y^\circ$	$+J_0 + K^\circ \beta_y^\circ$	0	$-J_1$	0	$+J_1$

Figure 13 Variation of Linear Acceleration due to Engine Forces with Time

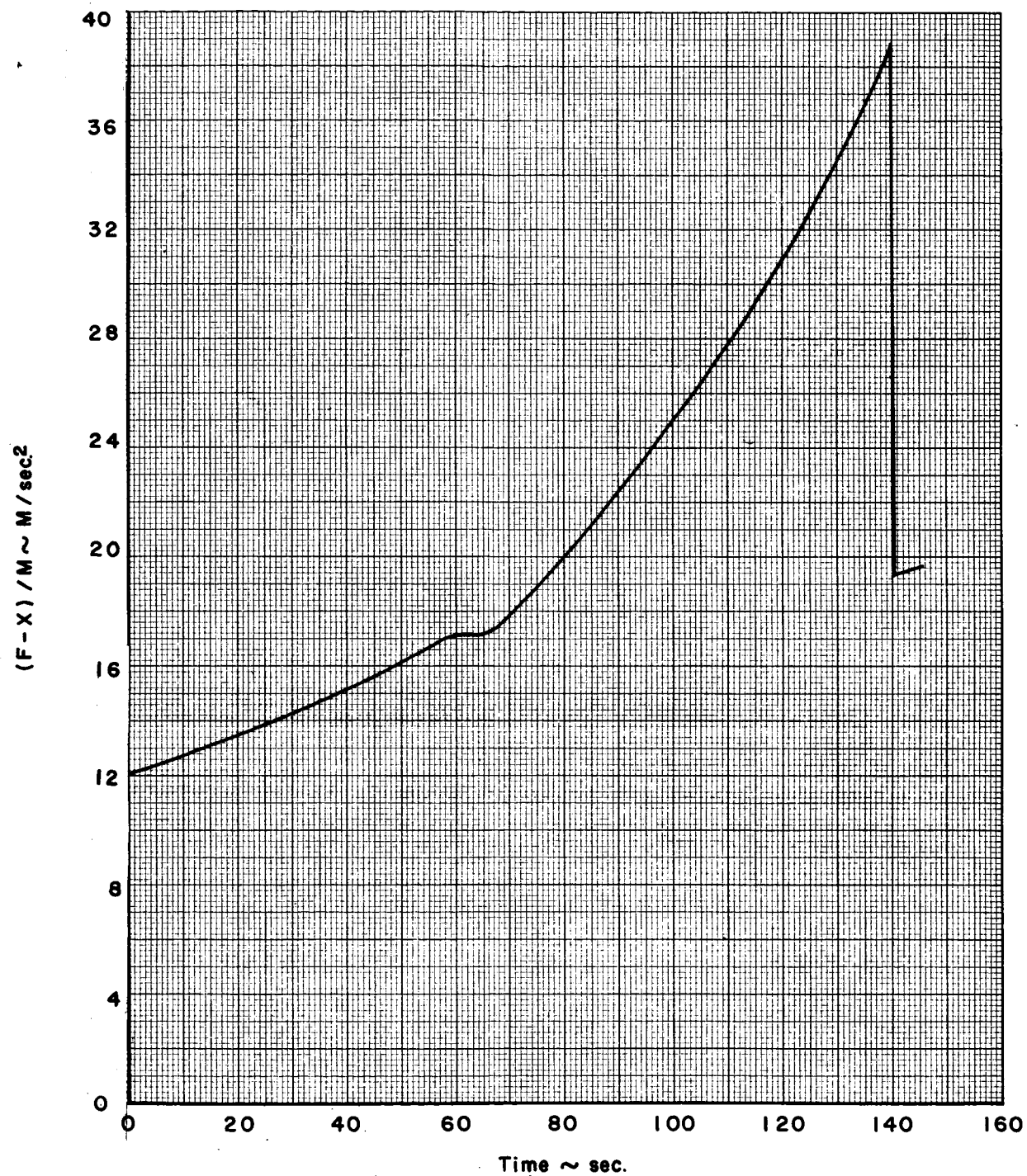


Figure 14 Variation of Resultant Axial Acceleration due to Aerodynamic and Engine Forces vs time

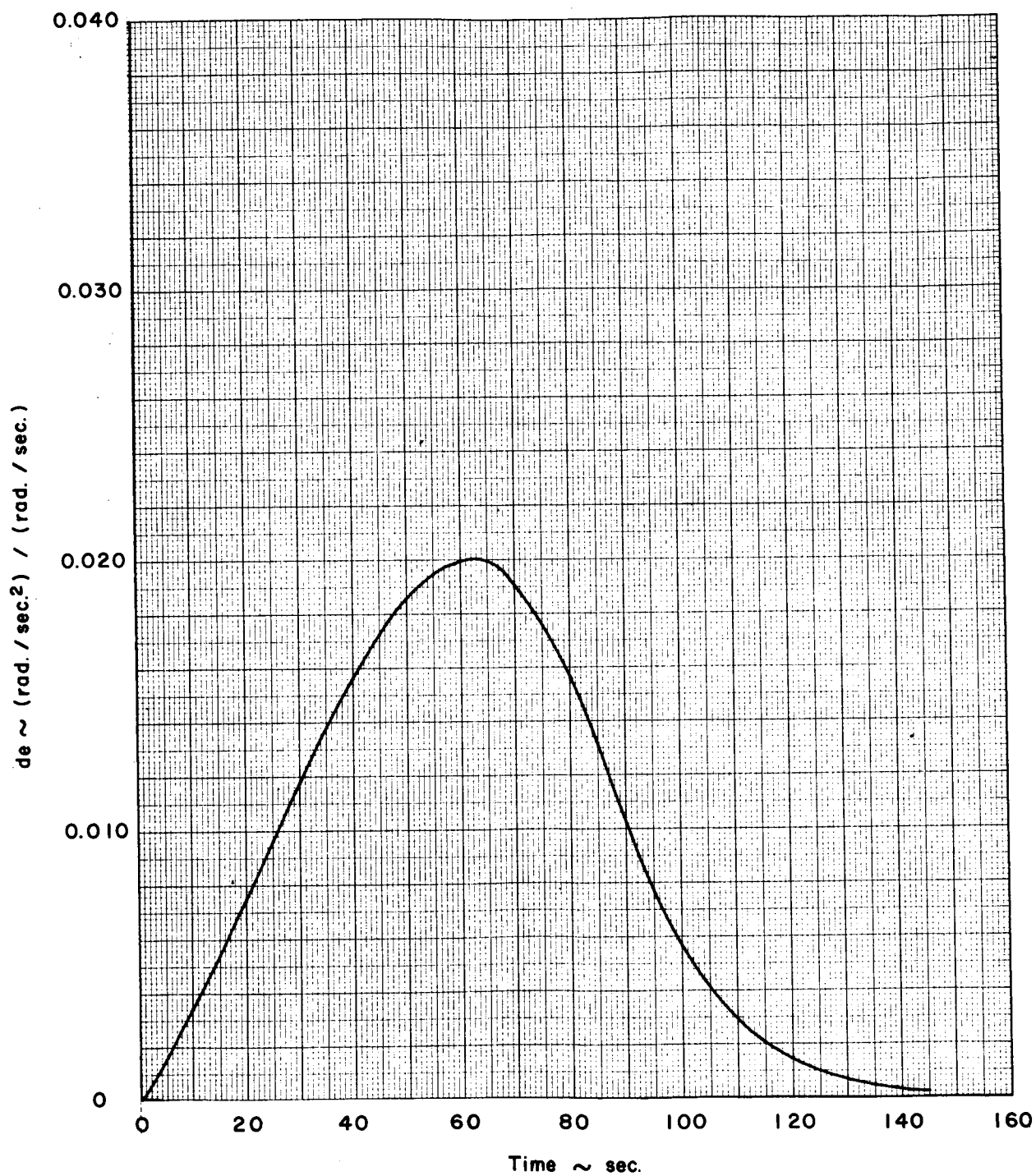


Figure 15 Variation of Angular Velocities due to Aerodynamic Forces vs Time

APPENDIX A*

CONTROL FACTOR SIGN CONVENTION

Sign Convention

The body-fixed coordinate system and sign convention chosen for control factor presentation are shown in Figure A-1. The coordinate system has its origin at the longitudinal location of the vehicle center of gravity with the x-axis being coincident with the vehicle longitudinal axis and positive in the forward direction. Looking in the positive x-direction, the y-axis points to the right and the z-axis points downward (see insert in Figure A-1). At lift-off the z-axis points downrange in the plane of flight. The three force components are identified by the direction in which they act: x = axial force component, y = side force component, and z = normal force component. The corresponding coefficients are C_x , C_y , and C_z . The moment components are called after the axis about which the vehicle may rotate: M_x = rolling moment, M_y = pitching moment, and M_z = yawing moment. The corresponding moment coefficients are C_{mx} , C_{my} , and C_{mz} . To facilitate the writing of a moment derivative by another subscript, the letters m, x, y and z are written on the same level; for example, $dC_{my}/d\alpha = C_{my}\alpha$. The directions of the positive force and moment coefficients are shown in Figure A-1.

The flow angles, i.e., angle of attack (pitch), angle of sideslip (yaw), and angle of roll, are defined by projecting the velocity vector onto the three principal planes of the coordinate system. The angle of attack (α) is inscribed between the projection of the flow vector \vec{V} onto the xz-plane and the positive part of the x-axis; α is positive when the z-component of \vec{V} points in the negative z-direction. The sideslip angle (τ) is inscribed between the projection of \vec{V} onto the xy-plane and the positive part of the x-axis; τ is positive when the y-component of the velocity vector points in the positive y-direction. The roll angle (ϕ) is inscribed between the projection of \vec{V} onto yz-plane and the positive part of the z-axis; ϕ is positive when measured clockwise from the \vec{V} projection to the positive part of the z-axis as viewed from the rear. With these sign rules of the flow angles, the following moment sign rules can be stated:

* The contents of this appendix are extracted from ABMA-DA-TN-27-60 [1].

+ M_x tends to make ϕ more positive
+ M_y tends to make α more positive
+ M_z tends to make τ more negative

} as viewed from
the space fixed
wind vector, \bar{V} .

All engine deflections are labeled β ; the deflection may then be further defined by a subscript corresponding to the direction of force that the deflection produces. Thus, β_z is an engine deflection which causes a force in the z-direction (normal force) and a moment about the y-axis (pitching moment); β_y is an engine deflection which causes a force in the y-direction (sideslip force) and a moment about the z-axis (yawing moment). The signs of β_z and β_y are positive if the engines so deflected produce a positive normal force or side force, respectively. The sign convention of all angles is also shown in Figure A-1.

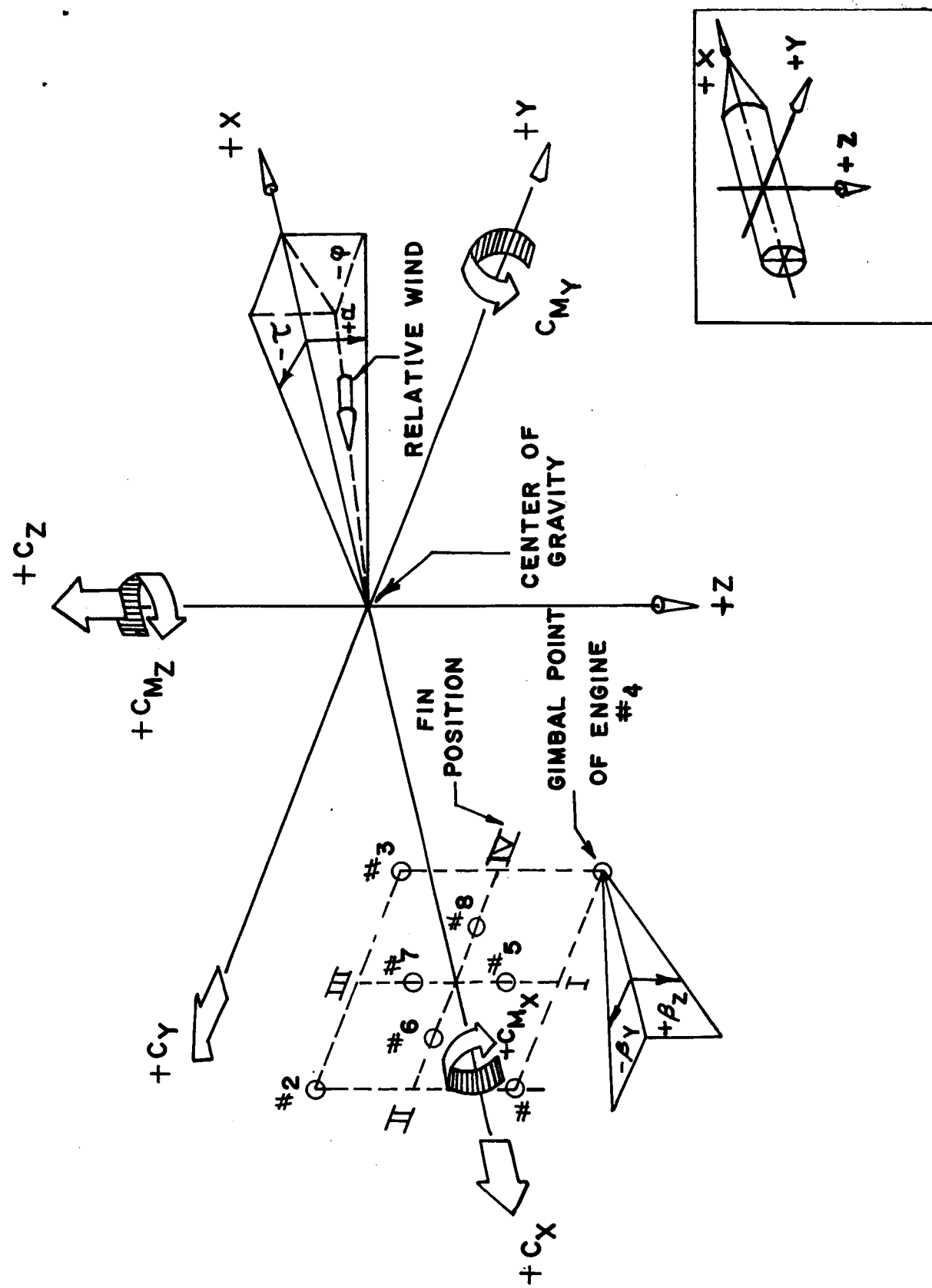


FIGURE A-1 SATURN VEHICLE ANGLE AND MOMENT SIGN CONVENTION

APPENDIX B

CONTROL FACTOR VARIATION BOUNDARIES

The control factor variations are obtained by the root-sum-square of the partial perturbations due to pertinent variants. The control factors thus treated are C_1 , C_2 , Z'_1/m , Z'_2/m , and corresponding ratios, C_1/C_2 , $(Z'_1/m)/Z'_2/m$, $C_1/(Z'_1/m)$, and $C_2/Z'_2/m$.

Because of interrelations between control factors, the VARIATIONS MUST BE USED WITH CAUTION. To illustrate, consider the following limitation: the MIN-MAX combinations of two control factors are not permissible. The reason for this restriction is illustrated in Figure B-1 using C_1 , C_2 , and C_1/C_2 .

(1) At a specified time point, the standard or nominal values of C_1 and C_2 are represented by a single point on the plot.

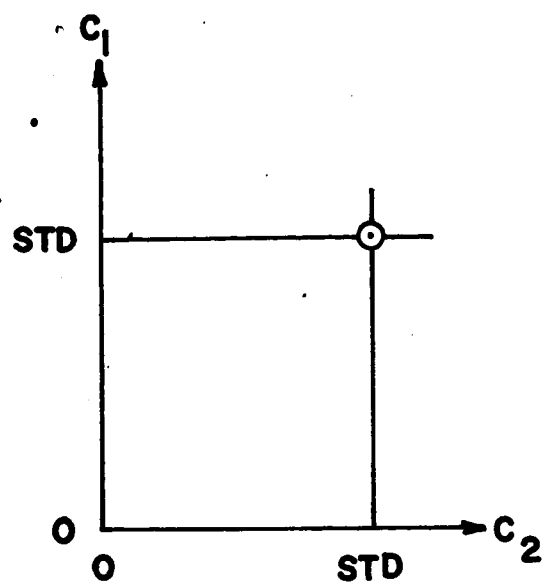
(2) From the tabulated data of the maximum and minimum values of C_1 and C_2 , the respective MAX and MIN lines may be added to the plot. Thus, we have drawn a box wherein possible combinations of C_1 and C_2 may exist for a specified sigma level.

(3) However, the box described above does not give a true boundary of the possible combinations of C_1 and C_2 . A concurrent C_1/C_2 analysis shows that it has MAX-MIN variations that lie within the MIN-MAX combinations of C_1 and C_2 . This is shown by the two rays through 0, 0 having MAX and MIN C_1/C_2 values. The nominal value is a ray passing through 0, 0 and $(C_1, C_2)_{\text{Std}}$.

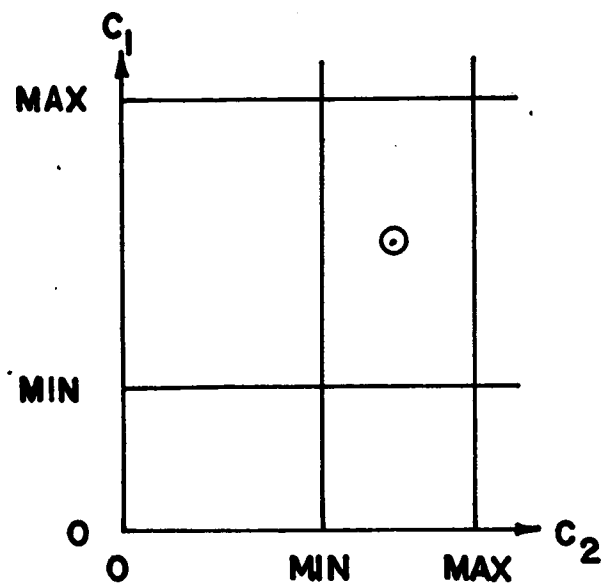
(4) The final boundary of a specified sigma level is shown here minus the construction lines.

Since C_1 , C_2 and C_1/C_2 are the most important factors in control, they were used in the illustration above. However, the technique is applicable to other combinations. A trace of C_1 and C_2 versus flight time is presented in the main body of the report, wherein one or more boundaries are shown for significant time points or as clarity of presentation permits.

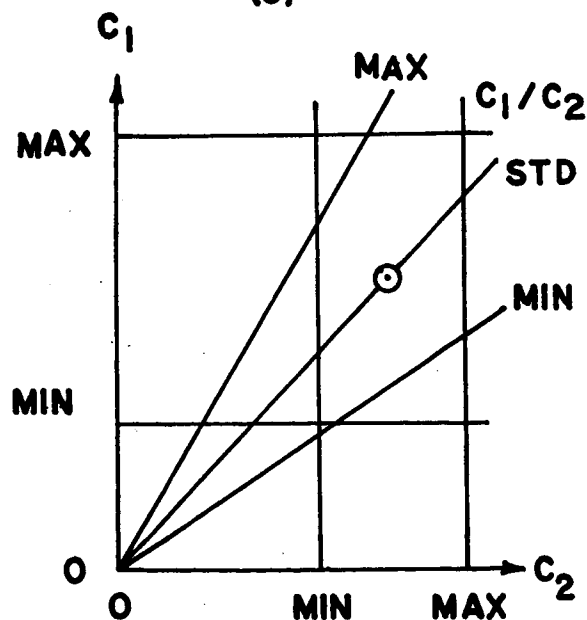
(1)



(2)



(3)



(4)

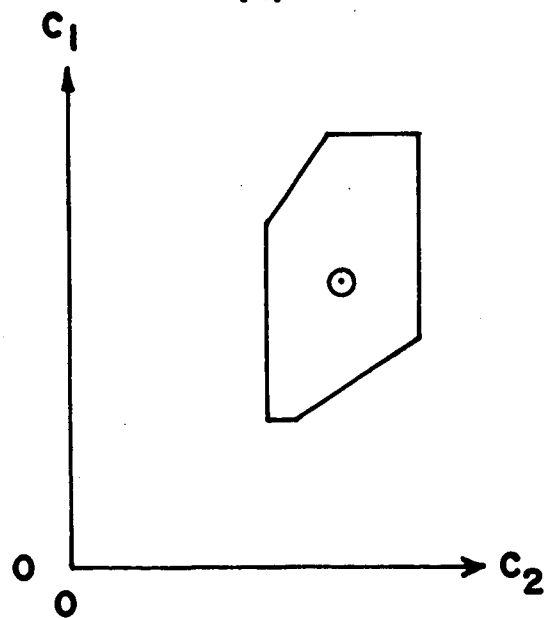


FIGURE B-1 CONSTRUCTION OF VARIATION BOUNDARIES

REFERENCES

1. Donehoo, Larry K., "Saturn Missile Control Factors: Sign Convention, Symbols, and Equations," ABMA-DA-TN-27-60, April 18, 1960, Unclassified.
2. Nunley, Billy W., "Design Criteria: Saturn IB/Apollo Operational Configuration Aerodynamic Axial Force Characteristics," R-AERO-AD-65-43, May 26, 1965, Unclassified.
3. Glover, J. C., "Saturn IB, SA-201, Preliminary Mass Characteristics Based on Projected Weights," R-P&VE-VAW-65-35, March 5, 1965, Confidential.
4. Advance Engineering Branch, "Dispersion Analysis and Flight Propellant Reserve Requirement for the Saturn IB, SA-201," CCSD-TB-AE-65-161, March 13, 1965, Unclassified.

July 19, 1965

APPROVAL

TM X-53296

CONTROL FACTORS FOR
APOLLO-SATURN 201 VEHICLE

By

Billy W. Nunley

The information in this report has been reviewed for security classification. Review of any information concerning Department of Defense or Atomic Energy Commission programs has been made by the MSFC Security Classification Officer. This report, in its entirety, has been determined to be unclassified.

This document has also been reviewed and approved for technical accuracy.

Bob G. Dunn

Bob G. Dunn
Chief, Design Section

Ellery B. May

Ellery B. May
Chief, Aerodynamic Design Branch

Werner K. Dahm

Werner K. Dahm
Chief, Aerodynamics Division

E. D. Geissler

E. D. Geissler
Director, Aero-Astrodynamic Laboratory

DISTRIBUTION

TM X-53296

DIR
Dr. von Braun

MS-IPL (8)

MS-IP

MS-H

HME-P

CC-P

MS-T (5)

R-AERO
Mr. Lindberg
Dr. Speer
Mr. Hagood
Mr. Stone
Mr. McNair
Mr. Teague
Mr. Dahm
Mr. Reed
Mr. Wilson
Mr. May
Mr. Dunn
Mr. Nunley
Mr. Andrews
Mr. Weaver

R-ASTR
Dr. Haeussermann
Mr. Moore
Mr. Schaefer
Mr. Mack
Mr. Hosenthien
Mr. Blackstone
Mr. Brandner
Mr. Richard
Mr. Griswold

EXTERNAL

Scientific and Technical Information Facility (25)
Attn: NASA Representative (S-AK/RKT)
P. O. Box 5700
Bethesda, Maryland

R-P&VE
Mr. Cline
Mr. Palaoro

Mr. John O. Windham
MSFC Resident Liaison Engineer
NASA, Langley Research Center
Langley Station, Bldg. 1218
Hampton, Virginia

RP
Mr. Spears

Mr. E. A. Rawls
Chrysler Corporation Space Division
Michoud Operations
Aerodynamics Group
P. O. Box 29200
New Orleans, Louisiana 70129

R-AERO
Dr. Geissler
Mr. Jean
Mr. Ryan
Mr. Horn
Mr. Winch
Mr. Verderame
Mr. Rheinfurth
Mr. Hall
Mr. Mowery
Mr. Lovingood